Solvation of a Flexible Biomolecule in the Gas Phase: The Ultraviolet and Infrared Spectroscopy of Melatonin−Water Clusters

Gina M. Florio and Timothy S. Zwier*

Department of Chemistry, Purdue University, West Lafayette, Indiana 47907-1393

Received: September 23, 2002; In Final Form: December 6, 2002

The neural hormone melatonin (*N*-acetyl-5-methoxytryptamine) is an indole derivative with a flexible peptide-like side chain that presents five distinct hydrogen-bonding sites for water: the carbonyl oxygen, the amide NH, the indole NH, the methoxy oxygen, and the indole π cloud. Using a combination of two-color resonant two-photon ionization (2C-R2PI), UV−UV hole-burning spectroscopy, and resonant ion-dip infrared spectroscopy (RIDIRS), the conformational preferences of melatonin upon sequential solvation with water have been examined. Density functional theory calculations are used to identify structural minima and to aid in the infrared spectral assignments. This work builds on previous results on the melatonin monomer (Florio et al. *J. Am. Chem. Soc.* **2002**, *124*, 10236), which identified five monomer conformations: three dominant *trans*-amide conformers and two minor *cis*-amide conformers. Four distinct melatonin−$(water)_1$ complexes and two melatonin−$(water)_2$ clusters are observed. All of these feature water binding to the carbonyl group as the primary point of attachment. The dominant two MEL−$(water)_1$ complexes retain the structures of the lowest energy monomer conformations, MEL(A, B). The other two structures (MEL−$(water)_1$ Y and Z) have water bound at the carbonyl group, but also perturb the indole NH stretch fundamental, suggesting that the water molecule interacts with both sites simultaneously. The infrared spectra of the two MEL−$(water)_2$ clusters point to a bridge structure joining the amide carbonyl and indole NH groups. The changes that occur in the potential energy landscape of melatonin in the presence of water will be discussed.

I. Introduction

Water plays a crucial role in directing the conformational preferences of molecules of biological relevance. Those water molecules in the first solvation shell are particularly important in this respect, often serving as bridges joining nearby hydrogen bonding sites on the solute. The study of biomolecule−$(water)_n$ clusters in the gas phase provides a unique vantage point for studying the effects of water complexation on the conformational preferences of small biomolecules.

Recent studies of this type have begun to consider molecules with several flexible coordinates and multiple H-bonding sites. In such cases, understanding the conformational preferences of the expansion-cooled, isolated molecule in the absence of water is already a task of substantial proportions. It is becoming clear that in order to understand why a molecule spreads its population over a certain number of conformations downstream in the expansion, one must consider not only the relative energies of the low-lying conformational minima but also the heights of the barriers separating all conformational minima carrying substantial population in the preexpansion mixture.[1−3]

We have recently carried out a study of the infrared and ultraviolet spectroscopy of the hormone melatonin, *N*-acetyl-5-methoxytryptamine (MEL), which contains a single, methyl-capped amide group.[3] This study identified transitions due to five conformers of MEL: three *trans*-amides that support the majority of the population (MEL A−C), and two minor *cis*-amide conformers (MEL D and E). The structures of these conformers are shown in Figure 1. The labels underneath the structures denote the position of the *N*-acetyl group relative to the indole ring: anti, gauche on the pyrrole side of indole (Gpy), and gauche on the phenyl side of indole (Gph). The amide configuration is given in parentheses (trans or cis), followed by a designation of the direction of the amide NH (in toward

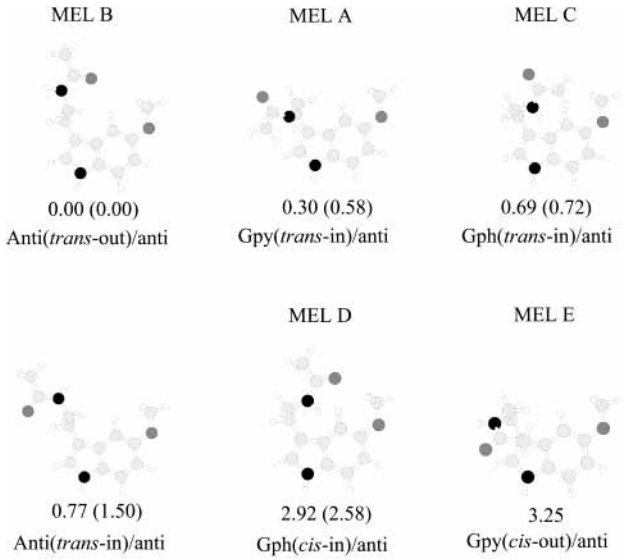

Figure 1. Six of the low-lying conformations of melatonin monomer calculated at the DFT Becke3LYP/6-31+G* level of theory. Conformers A−E were observed experimentally (ref 3). The Anti (*trans*-in)/anti structure is included to show the energetic consequences of reorienting the *trans*-amide group about the C(α)−N bond. The DFT zero-point corrected relative energies in kcal/mol are displayed beneath each structure, with localized MP2/aug-cc-pVTZ(-f) single-point energies listed in parentheses, taken from ref 3.

* Corresponding author. E-mail: zwier@purdue.edu. Phone: (765) 494-5278. Fax: (765) 494-0239.

10.1021/jp027053i CCC: $25.00
Published on Web 01/23/2003

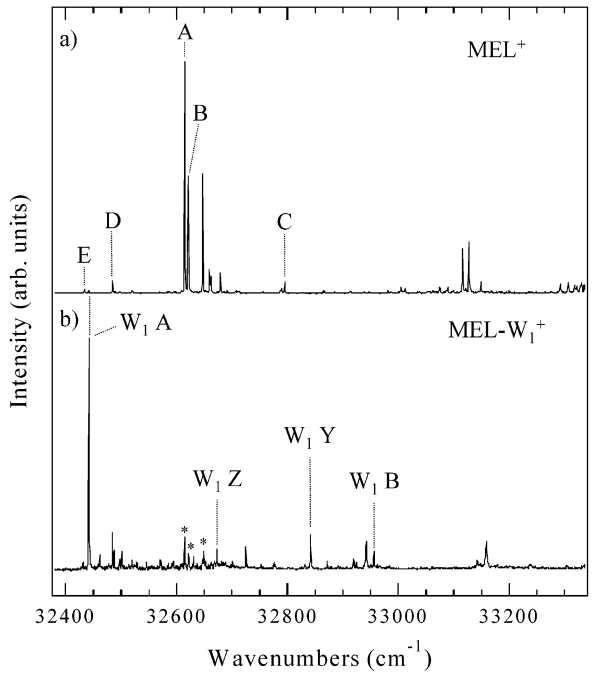

Figure 2. Two-color resonant two-photon ionization scans monitoring the (a) MEL monomer mass channel and (b) MEL−$(H_2O)_1^+$. The transition labeling identifies the S_0-S_1 origin transitions of the five MEL monomer conformations (A−E) and four MEL−$(H_2O)_1$ conformations observed. The asterisks in (b) show false transitions appearing at the positions of the strong transitions of MEL monomer, ringing into the time window gated on for the MEL−$(H_2O)_1$.

the phenyl ring or out away from it). Finally, the syn/anti designation refers to the orientation of the (in-plane) methoxy group relative to the indole NH. Only anti methoxy structures are observed.

Figure 2a shows the 2C-R2PI spectrum of MEL monomer, with the $S_1 \leftarrow S_0$ origins of the five conformers labeled with letters corresponding to the assigned structures from Figure 1. The *cis*-amide conformers are calculated to be about 3 kcal/mol higher in energy than the lowest energy *trans*-amide conformers. Population is trapped in these conformers due to the large barrier (∼15 kcal/mol) associated with *cis*−*trans* amide isomerization.

Melatonin possesses several H-bonding sites for attachment of water. Water can act as a H-bond donor to the amide carbonyl, methoxy oxygen, or indole π clouds, while it can accept a H-bond from the amide NH and indole NH groups. When one or more water molecules bind to such a molecule, a first question of interest is simply to establish where water will prefer to bind. Second, one would like to establish how this binding changes the conformational preferences of the molecule. Finally, one would hope to follow this interplay between solvation and conformational preferences as the number of water molecules grows.

Two recent studies have reported on the photophysics and spectroscopy of melatonin in solution.[4,5] The fluorescence quantum yields remain quite high even in aqueous solution ($\phi_f \sim 0.1$). Unlike tryptophan,[6] the fluorescence decay is single-exponential, and shows little change in its absorption maximum in different solvents. The fluorescence of MEL in aqueous solution is red-shifted (356 nm at pH 7) compared to all other solvents (332−336 nm). This red shift has been attributed to the stabilization of the excited state due to H-bonding between water and the indole NH.

This paper describes the infrared and ultraviolet spectroscopy of melatonin−$(water)_n$ clusters containing one or two water molecules. The same double-resonance methods that play such an important role in the recent studies of MEL monomer[3] are employed in the present work, among them two-color resonant two-photon ionization (2C-R2PI), UV−UV hole-burning spectroscopy, and resonant ion-dip infrared spectroscopy (RIDIRS).[7] As we shall see, there are four conformers of the melatonin−$(water)_1$ complex, all of which are bound at the amide carbonyl group. Two of the minor conformers of melatonin−$(water)_1$ show evidence of forming a bridge between the indole NH and amide carbonyl groups. Two conformers of melatonin−$(water)_2$ are identified, both of which appear to form a water dimer bridge between the amide carbonyl and the indole NH groups.

II. Methods

A. Experimental Methods. The experimental methods used in this study have been recently reviewed.[7] Melatonin (MEL) was obtained commercially (97% pure, Sigma) and used without further purification. Molecular clusters were formed in a supersonic expansion from a heated MEL sample (470 K) in a 3 bar, 70% neon/30% helium/0.1% water gas mixture. This mixture was pulsed into a differentially pumped vacuum chamber at 20 Hz, using a pulsed valve (General, series 9, 0.8 mm diameter). The expansion is skimmed ∼3 cm downstream from the nozzle orifice, and mass-analyzed by time-of-flight mass spectrometry.

This work employs spectroscopic methods that are based on mass selected two-color R2PI spectroscopy. To obtain the two-color R2PI (2C-R2PI) spectra of jet-cooled MEL−$(water)_n$, the doubled output of a Nd:YAG-pumped dye laser operating at 20 Hz was used to probe the $S_1 \leftarrow S_0$ transition. Typical unfocused UV output is 200 μJ/pulse using rhodamine 610 in methanol, rhodamine 640 (oscillator) and rhodamine 610 (amplifier) in ethanol, or sulforhodamine 640 in methanol. The third harmonic of a Nd:YAG laser (355 nm, ∼1 mJ/pulse) was used for the ionization step, $D_0 \leftarrow S_1$. The 355 nm laser was spatially and temporally overlapped with the UV laser. 2C-R2PI was used instead of one-color R2PI because it provided enhanced ionization efficiency with little detectable fragmentation. Cannington and Ham[8] report the vertical ionization potential of MEL as 7.7 eV, with an approximate value of 7.03 eV for the adiabatic ionization threshold. Since ionization is localized on the indole ring, the adiabatic ionization threshold of the monomer serves as a likely approximate measure of the ionization energy for the water-containing clusters studied here. Using this value for the ionization potential, 2C-R2PI gives the clusters about 4000 cm^{-1} of excess energy, versus about 8500 cm^{-1} of excess energy in the 1C-R2PI scheme at the S_1 origin.

In the case of flexible molecules and molecular clusters, mass analysis by itself cannot separate the various conformational isomers present in the R2PI spectrum. The double-resonance technique of UV−UV hole-burning spectroscopy was used to obtain R2PI spectra of individual MEL−$(water)_n$ conformational isomers, free from interference from one another. The UV−UV hole-burning spectra were obtained by fixing the hole-burning UV laser (10 Hz) on the origin transition of a particular MEL−$(water)_n$ cluster conformation and tuning a time-delayed probe UV laser (20 Hz) through the R2PI spectrum, while monitoring the difference in mass-selected ion signal with and without the hole-burning laser present. Using active base-line subtraction, all of the vibronic transitions that arise from the same ground-state level as the hole-burned origin transition show up as depletions in the hole-burning spectrum.

Infrared spectra in the hydride-stretch region of individual MEL−$(water)_n$ clusters were obtained using a second double

resonance technique, which we refer to as resonant ion-dip infrared spectroscopy (RIDIRS).[7] For such scans, the infrared output (2200−4000 cm^{-1}) of an injection seeded Nd:YAG-pumped optical parametric converter was spatially overlapped with the two R2PI lasers, preceding them by 50−200 ns. 2C-R2PI, with λ_1 fixed to a given cluster $S_1 \leftarrow S_0$ origin, generates a constant ion signal in the MEL−$(water)_n^+$ mass channel due to a single MEL−$(water)_n$ cluster conformation. The IR laser is operated at 10 Hz and tuned through the hydride-stretching region, removing population out of the ground vibrational level whenever it is resonant with a vibration in the cluster of interest. Using active base-line subtraction, infrared transitions in the selected ground-state MEL−$(water)_n$ conformation are detected as depletions in the ion current.

B. Calculations. In our previous study on the conformational preferences of MEL in the absence of water,[3] we performed a thorough search of conformational space using the OPLS-AA force field, followed by Hartree−Fock optimizations, density functional theory optimizations, and localized MP2 single-point energy calculations. These optimized monomer structures serve as reasonable starting points for the calculation of MEL−$(water)_n$ cluster conformations. Additional MEL conformations that are not minima in the absence of water have also been considered in the present work.

Density functional theory (DFT) calculations employing the Becke3LYP functional[9,10] with a 6-31+G*(5d) basis set[11] have been carried out to provide a basis of comparison with the experimental results on the MEL−$(water)_1$ clusters. The fully optimized structures, vibrational frequencies, IR intensities, and binding energies were computed for various potential structures of MEL−$(water)_1$. All calculations were performed using the Gaussian 98 suite of programs.[12]

Binding energies were calculated for all minimum energy structures in the following manner. The binding energy of a MEL−W_1 complex is defined as

$$\mathrm{BE} = E_{\mathrm{cluster}} - E_{\mathrm{monomer}} - E_{\mathrm{water}}$$

where the energies of the cluster, monomer, and water are the fully optimized, zero-point-corrected energies of each species at the same level of theory. In the case of flexible molecules, the structure of the monomer in the cluster geometry can be very different from the monomer in the absence of water. It is possible that water can stabilize structures of the monomer that are not even minima on the monomer potential energy surface in the absence of water. The flexibility of molecules such as MEL makes the definition of binding energies for the MEL−$(water)_n$ cluster somewhat ambiguous. In the results section (Table 1), the binding energies are listed in one of several ways. When comparing the energy of the complex to a single reference monomer energy, we have used the calculated lowest-energy structure of the monomer, Anti(*trans*-out)/anti. It should be noted that this structure is the one assigned to MEL B, and not MEL A, and as such is the second lowest energy conformation according to experiment. For clusters based on monomer structures that are optimized minima in the absence of water, we have also calculated the binding energy using the energy of the corresponding fully optimized monomer structure. Finally, when the formation of the complex contorts the MEL structure away from any minimum in the absence of water, single-point calculations at that structure have also been used to provide a third reference. The difference between these latter two binding energies gives a measure of the internal strain of the monomer in the complex.

TABLE 1: Calculated Binding Energies (kcal/mol) of the Melatonin−$(Water)_1$ Complexes

structure	BE (Anti(*trans*-out)/anti)[a]	BE (optimized monomer)[b]	BE (SP monomer)[c]	strain energy[d]
I	6.71	7.47	7.96	0.49
II	5.91		8.85	
III	5.88	6.18	7.75	1.57
IV	5.73	5.73	6.00	0.26
V	5.62		8.13	
VI	5.56	5.86	6.24	0.38
VII	5.46	5.76	6.50	0.74
VIII	4.94	5.25	5.87	0.62
IX	4.88	8.13	9.81	1.68
X	4.73	5.03	5.18	0.15
XI	4.65	8.11	8.51	0.39
XII	2.73	3.49	3.74	0.24

[a] Binding energy relative to the Anti(*trans*-out)/anti melatonin conformer A. [b] Binding energy relative to the monomer minimum associated with the water cluster. [c] Binding energy relative to the monomer held fixed in the cluster geometry (based on a single-point calculation). [d] Difference between the binding energy calculated relative to the optimized monomer (column 3) and the monomer in the cluster geometry (column 4).

For each cluster, we have also corrected the binding energy for zero-point effects. As with the binding energies, the zero-point energy corrections of the monomers are ambiguous when there is substantial distortion of the monomer upon complex formation away from a minimum. The single-point monomer energies were corrected for zero-point contributions using the average zero-point energy of the fully optimized MEL monomers, 172.28 ± 0.11 kcal/mol. For clusters based on stable monomer species, calculating the binding energy using the single-point energy and the average zero-point energy deviates from the standard method by less than 10% in all cases.

III. Results and Analysis

A. Calculated Structures, Energetics, and Infrared Spectra. Figure 3 shows the fully optimized structures of twelve distinct MEL−$(water)_1$ species, hereafter referred to as MEL−W_1, labeled with their zero-point corrected energy, relative to the global minimum. The energetics of these structures are summarized in Table 1. These structures are just a small number of the total feasible MEL−W_1 structures, but include water bound to all of the major H-bonding sites of MEL, except the methoxy oxygen. To assess the strength of the H-bond between water and the methoxy oxygen, calculations were performed on the 5-methoxyindole−W_1 (5-MOI−W_1) cluster. The calculated MEL−W_1 structures show water bound only to the carbonyl (structures **I**, **III**−**V**, **VII**), only the amide NH (structure **XII**), only the indole NH (structure **X**), and several structures where water is bridging between two H-bonding sites of MEL (structures **II**, **VI**, **VIII**, **IX**, and **XI**). All of the MEL−W_1 structures are within ∼2 kcal/mol of each other, with the exception of the amide NH-bound Anti(*trans*-in)/anti-W_1 cluster (+4.00 kcal/mol). The notation used here is based on that developed for the MEL monomers, and is defined as backbone position(amide NH orientation)/methoxy position and "in" or "out" refers to whether the amide NH is pointed in toward or out away from the indole ring. Some of the structures in Figure 3 are based on monomer species that are observed in the expansion prior to the introduction of water (Figure 1): Gpy(*trans*-in)/anti (structures **III**, **VIII**, and **IX**), Anti(*trans*-out)/anti (structure **IV**), Gph(*trans*-in)/anti (structure **VII**), and Gpy(*cis*-out)/anti (structure **IX**). Only MEL and 5-MOI structures with anti-oriented methoxy groups were considered for

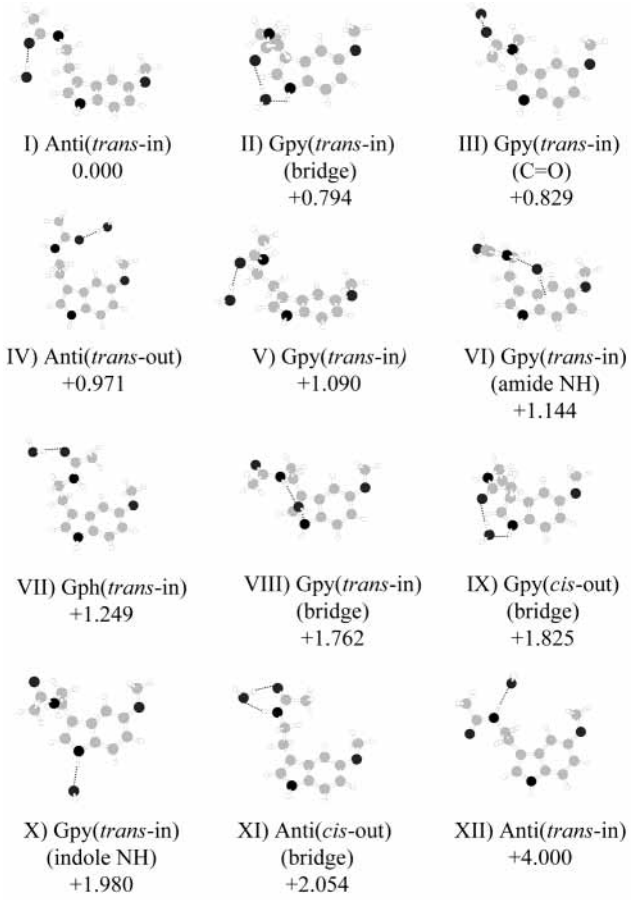

Figure 3. Twelve low-energy structures of MEL−$(H_2O)_1$ calculated at the DFT Becke3LYP/6-31+G*(5d) level of theory. The relative energies (in kcal/mol) are displayed beneath each structure, together with a short-hand notation used to label the conformers (see text). The structures illustrate various types of structures, and should not be considered exhaustive.

the MEL−W_1 and 5-MOI−W_1 calculations. The orientation of the methoxy group was discussed in detail in the previous MEL monomer study,[3] and it was determined that MEL and 5-MOI prefer conformations with the methoxy group oriented anti with respect to the indole NH by about 3 kcal/mol.

The DFT Becke3LYP/6-31+G*(5d) calculations cannot reliably distinguish between close-lying structures based on energetics alone, due to the modest basis set used and to the improper accounting of dispersion inherent to DFT. Nevertheless, many of the major trends observed in these calculations are expected to hold at higher levels of theory. The global minimum of the DFT calculations is structure **I**, in which water is bound to the carbonyl of the Anti(*trans*-in)/anti monomer conformation. The Anti(*trans*-in)/anti monomer is predicted to be the fourth lowest energy structure at +0.77 kcal/mol by the DFT method, and is not observed in the expansion in the absence of water. The lowest energy monomer species is calculated to be the Anti-(*trans*-out)/anti structure, but it has been assigned to MEL conformer B (the second most populated monomer experimentally) based on its infrared spectral signatures.[3] The Anti(*trans*-out)/anti structure differs from the Anti(*trans*-in)/anti structure primarily by 180° rotation about the C(α)−N bond, the barrier for which is estimated to be less than 2 kcal/mol by single-point DFT calculations at the same level of theory. According to the calculations, the addition of water at the carbonyl group lowers the Anti(*trans*-in)/anti conformer relative to the Anti-(*trans*-out)/anti conformer, presumably due to a stabilizing interaction between the water and the pyrrole CH.

In the absence of a second stabilizing H-bond, the DFT calculations predict that the amide carbonyl group is the preferred H-bonding site for water (structures **I**, **III**−**V**, and **VII**), where it acts as a H-bond donor. Water can act as an acceptor at either the indole NH or amide NH. The former site is bound by about 2 kcal/mol less (structure **X**), while the amide NH is a surprisingly poor donor to water (structure **XII**), with a binding energy some 4 kcal/mol less than structure **I**. Finally, the methoxy group is also predicted to be a poor H-bond acceptor, based on the small calculated binding energy of the 5-MOI−W_1 cluster (D_0 = 3.56 kcal/mol).

We have shown previously the importance of water bridge formation in directing the conformational preferences of flexible molecules such as tryptamine (TRA) and 3-indole-propionic acid (IPA).[13] In keeping with this, several MEL−W_1 bridges have been identified by the DFT calculations where the water molecule behaves as both a H-bond donor and acceptor (structures **II**, **VI**, **VIII**, **IX**, and **XI**). The formation of a water bridge with two H-bonds linking sites on MEL leads to total binding energies that can begin to compete with the strong carbonyl binding. However, to form this bridge, the flexible side-chain of MEL must take on conformations that close the gap between the two sites, thus introducing conformational strain that must be compensated by the increased binding energy of the bridge. For example, structures **VI** and **VIII** incorporate a water bridge between the amide NH and the indole π cloud, and are only 1.1 and 1.8 kcal/mol less stable than the global minimum. Water bridging across the *cis*-amide group (structure **XI**) trades off the destabilization of the *cis*-amide group for stronger binding of water across the amide NH and C=O sites.

The lowest energy bridge structure (structure **II**, +0.79 kcal/mol) is based on a gauche pyrrole *trans*-amide structure that was not identified as a minimum in the absence of water. The water bridge in structure **II** has the water donating a H-bond to the carbonyl group and accepting a H-bond from the indole NH. In contrast to gauche pyrrole structures that are low-energy minima in the monomer, the carbonyl group of MEL in structure **II** is gauche with the pyrrole ring of indole, the amide NH is pointed up away from the indole π cloud, and the side chain is nearly perpendicular to the indole ring. The H-bond between the indole NH and water forces the indole NH out of plane by about 16°, thereby maximizing the H-bonding interaction.

Structure **IX** is essentially identical to structure **II**, but with a cis oriented amide group, and is almost 1 kcal/mol higher in energy (+1.76 kcal/mol). Structures **VI** and **VIII** are W_1 bridges based on the Gpy(*trans*-in)/anti monomer species, with the water molecule accepting a H-bond from the amide NH and donating a H-bond to the π cloud (VI) or the indole nitrogen (VII). The orientation of MEL in structure **VIII** is nearly identical to the monomer structure in the absence of water, while structure **VI** exhibits a slight rotation of the *N*-acetyl group about the C(α)−N bond, pointing the amide NH up away from the indole π cloud. Finally, structure **XI** is a W_1 bridge across the *cis*-amide group of an Anti(*cis*-out)/anti MEL species, where the water accepts a H-bond from the amide NH and donates one to the C=O. This is similar to the arrangement of the water molecule found in 1:1 clusters with the ring-constrained cis amide configurations present in 2-pyridone[14−16] and oxindole.[17] For MEL, water bridging across the *cis*-amide group is the highest energy bridge structure because it necessitates a *trans*−*cis* amide isomerization.

The harmonic vibrational frequencies and infrared intensities of the MEL−W_1 and 5-MOI−W_1 clusters have been calculated using the Becke3LYP/6-31+G*(5d) method. The calculated infrared spectra have aided the structural assignment of the

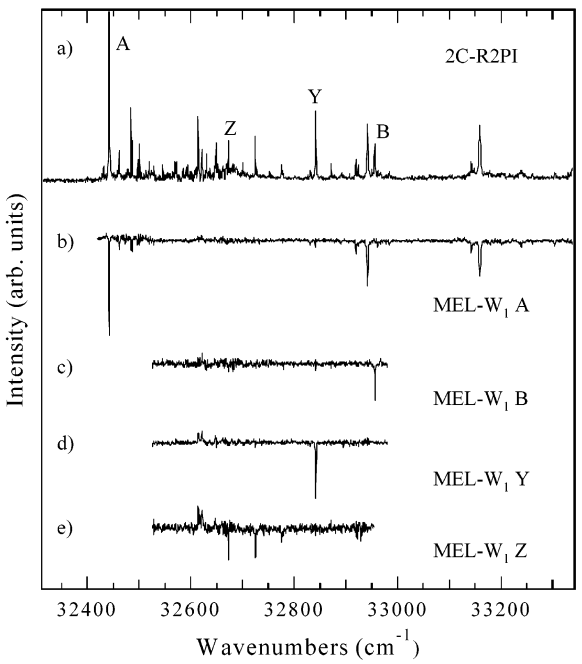

Figure 4. (a) Two-color R2PI spectrum and (b−e) UV−UV hole-burning spectra taken with the hole-burning laser tuned to the transitions labeled with the appropriate conformational label in (a). The hole-burning spectra divide the R2PI spectrum into its constituent pieces due to each of the conformations present, identifying four conformations of MEL−W_1.

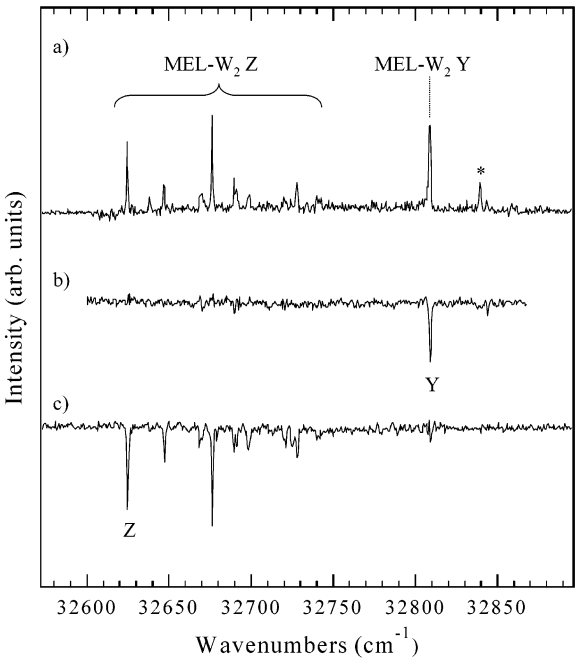

Figure 5. (a) Two-color R2PI spectrum and (b and c) UV−UV hole-burning spectra taken with the hole-burn laser tuned to transitions Y and Z, respectively, establishing that all observed transitions of MEL−W_2 belong to one of two conformations (Y and Z). A small transition at 32844 cm^{-1} (labeled with an asterisk in Figure 5a) is unaccounted for in the hole-burning spectra, and is possibly the origin of a third minor MEL−W_2 species. There was insufficient ion signal to perform either UV−UV hole-burning or RIDIRS on this transition.

experimentally observed MEL−W_1 clusters. For brevity's sake, the harmonic vibrational frequencies and infrared intensities of the relevant structures are included in the Supporting Information.

B. 2C-R2PI and UV−UV Hole-Burning Spectroscopy of MEL−W_1. The 2C-R2PI spectrum obtained in the MEL−W_1^+ mass channel, $m/z = 250$ (Figure 2b), is dominated by a transition at 32442 cm^{-1}, labeled MEL−W_1 A, with a frequency shift of −172 cm^{-1} from the MEL A origin. There are a number of bands to the blue of the MEL−W_1 A transition that could be vibronic structure of MEL−W_1 A, other MEL−W_1 species, and/or fragments from larger MEL−$(water)_n$ clusters, necessitating double-resonance methods of UV−UV hole burning and RIDIRS to determine the nature of these transitions. There are also false peaks in the R2PI spectrum due to ringing from transitions in the MEL monomer mass channel, which are marked by asterisks in the figure.

The UV−UV hole-burning spectra of MEL−W_1 species (Figure 4b−d) are compared to the 2C-R2PI spectrum in Figure 4a. The hole-burning spectrum of MEL−W_1 A (Figure 4b) was obtained with the hole-burn laser fixed to the vibronic transition at 32942 cm^{-1}. The hole-burning spectra of MEL−W_1 B (Figure 4c), W_1 Y (Figure 4d), and W_1 Z (Figure 4e) were obtained with the hole-burn laser fixed on the cluster origin transitions at 32956, 32842, and 32673 cm^{-1}, respectively. UV−UV hole-burning spectroscopy proves that the 2C-R2PI signal obtained in the MEL−W_1^+ mass channel consists of at least four distinct species. The MEL−W_1 A hole-burning spectrum shows a significant amount of vibronic structure within 85 cm^{-1} of the origin transition, due to both intermolecular vibrations and low frequency motions of the MEL side chain, which are difficult to assign and are probably mixed in character. The strong vibronic transition at +500 cm^{-1} in the MEL−W_1 A spectrum is observed in MEL A, MEL B, and other indole derivatives, and is due to a C═C/C−C stretching vibration in the aromatic ring. The other intense transition in the MEL−W_1 A spectrum occurs at +717 cm^{-1}, similar to that observed in indole.[18] The hole-burning spectra of MEL−W_1 B and Y show no vibronic structure over the frequency range scanned, while the MEL−W_1 Z spectrum is dominated by a progression in a 52 cm^{-1} vibration along with some additional weaker vibronic structure.

C. 2C-R2PI and UV−UV Hole-Burning Spectroscopy of MEL−W_2. The 2C-R2PI spectrum obtained in the MEL−W_2^+ mass channel, $m/z = 268$, is shown in Figure 5a. All of the structure observed in the MEL−W_2^+ mass channel occurs between 32620 and 32845 cm^{-1}, blue shifted from the MEL A, B, and C monomer origin transitions and in the same region as that of the MEL−W_1 B, Y, and Z cluster origins. Solely on basis of the position of the transitions in the MEL−W_2^+ mass channel, we would predict that the MEL−W_2 cluster(s) might be associated with the MEL−W_1 B, Y, and Z clusters. Again, double-resonance spectroscopy is needed to determine the number of W_2 species and their structures. Comparison of the 2C-R2PI spectra in MEL−W_1^+, MEL−W_2^+, and MEL−W_3^+ (not shown) indicates that no significant fragmentation is occurring among these mass channels under 2C-R2PI conditions with low water flow. The only observable fragmentation is of the MEL−W_1 A complex into the MEL^+ mass channel at its origin transition (32442 cm^{-1}), but even here, the magnitude of the ion signal in the monomer mass channel was less than 10% of the total MEL−W_1 A ion signal.

The UV−UV hole-burning spectrum obtained with the hole-burn laser fixed on the transition at 32814 cm^{-1} (labeled MEL−W_2 Y) is shown in Figure 5b, while that with the hole-burn laser fixed at 32629 cm^{-1} (MEL−W_2 Z) is shown in Figure 5c. The 2C-R2PI spectrum cleanly divides into spectra due to two major W_2 species. MEL−W_2 Y has a strong origin transition, but no observable vibronic structure. MEL−W_2 Z shows a clear progression in a 52 cm^{-1} vibration, closely analogous to that observed in MEL−W_1 Z, suggesting that this

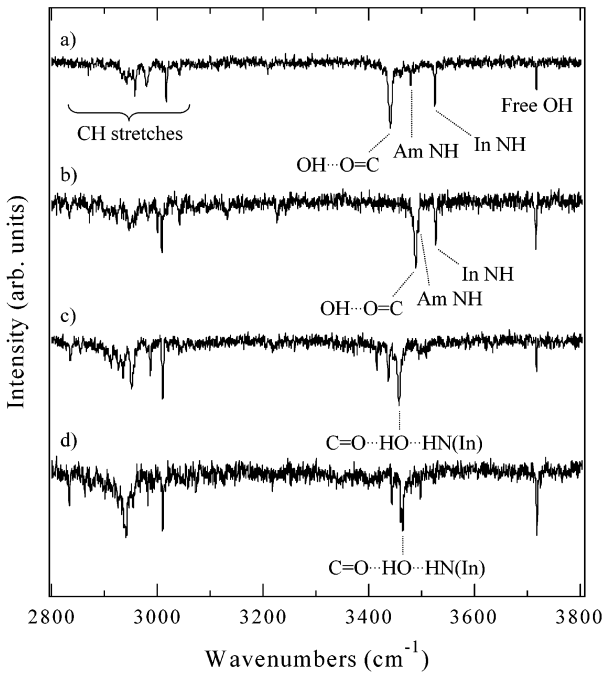

Figure 6. Resonant ion-dip infrared spectra monitoring the ion signal due to conformers (a) A, (b) B, (c) Y, and (d) Z of MEL−W_1.

is a W_2 cluster built off of MEL−W_1 Z. The nature of the 52 cm^{-1} vibration is probably a low-frequency vibration of the MEL side chain, and not an intermolecular vibration, because its frequency and intensity pattern in the progression are unchanged upon addition of a second water molecule. The origin of MEL−W_2 Z is shifted −44 cm^{-1} from that of MEL−W_1 Z. Assuming that MEL−W_1 Z and MEL−W_2 Z are associated, it is plausible that MEL−W_2 Y is built off of MEL−W_1 Y in a similar way, due to the notable lack of vibronic structure in each cluster's R2PI spectrum and the 28 cm^{-1} red-shift of MEL−W_2 Y with respect to MEL−W_1 Y. We will show that RIDIRS also supports these associations.

D. RIDIRS of MEL−W_1. Figure 6a−d shows the RIDIR spectra of the four MEL−W_1 clusters in the CH, NH, and OH stretching regions (2800−3800 cm^{-1}). The frequencies of the RIDIR transitions are summarized in Table 2. The RIDIR spectra obtained for the MEL−W_1 clusters are all consistent with water donating a single H-bond to the carbonyl of MEL, thereby producing one intense, broad transition located between 3441 and 3490 cm^{-1} corresponding to the OH···O═C hydride stretch. The OH···O═C stretch position in the MEL−W_1 clusters compares well with the known C═O bound W_1 clusters of tropolone[19] at 3506 cm^{-1} and *trans*-formanilide (TFA)[20,21] at 3515/3537 cm^{-1}. In the RIDIR spectra of all the MEL−W_1 complexes, a free OH stretch is observed at about 3717 cm^{-1} (Table 2). On the basis of the presence of a free OH stretch and a H-bonded OH stretch, we conclude that water is donating only one H-bond in these clusters.

MEL−W_1 A and B both show free amide NH and indole NH stretches, indicating that the water molecule is not bound at either of these positions. Thus, MEL−W_1 A and B are complexes in which the water is bound only to the C═O group of the side chain. As in the MEL monomers, the position of the amide NH stretch in these MEL−W_1 clusters is a sensitive probe of the orientation of the MEL side chain with respect to the indole ring. In our previous work on MEL monomer,[3] it was determined that for *trans*-amide MEL monomers (MEL A−C), the three lowest energy conformations have the side chain oriented gauche with respect to the pyrrole ring (MEL A), gauche with respect to the phenyl ring (MEL C), and pointing away from (or anti to) the indole ring (MEL B), as shown in Figure 1. The anti-oriented side chain conformation (MEL B) possesses an amide NH stretch fundamental at 3495 cm^{-1}. For the gauche configurations (MEL A and C), the amide NH stretch shows a slight red shift to ∼3480 cm^{-1} due to a weak interaction of the NH with the indole π cloud. The amide NH stretch in the MEL−W_1 A conformer occurs at 3479 cm^{-1} and the amide NH stretch of MEL−W_1 B is at 3494 cm^{-1}, indicating that MEL−W_1 A has a gauche oriented side chain and MEL−W_1 B has an anti oriented side chain.

As shown in the close-up scans of Figure 7, the free amide NH and indole NH stretches of MEL−W_1 A and MEL−W_1 B appear at nearly identical frequencies to the corresponding amide NH stretch fundamentals in the MEL A (Figure 7a) and B (Figure 7c) monomer species. This leads to the conclusion that MEL−W_1 A (Figure 7b) is associated with MEL A and MEL−W_1 B (Figure 7d) is associated with MEL B. Previously, we assigned MEL A to the Gpy(*trans*-in)/anti conformer and MEL B to the Anti(*trans*-out)/anti conformer.[3] We therefore assign MEL−W_1 A to water bound to the carbonyl of the MEL A Gpy(*trans*-in)/anti conformer (structure **III**), and MEL−W_1 B to water bound to the carbonyl of the MEL B Anti(*trans*-out)/anti conformer (structure **IV**).

These assignments are strengthened by the fact that MEL A and MEL B are the two most abundant monomer conformers observed in the supersonic expansion, with populations of 0.66 and 0.23, respectively.[3] In keeping with this, the MEL−W_1 A cluster is the most abundant W_1 species, with a population estimated to be about 10 times greater than that of any other W_1 species observed in the expansion. Finally, the calculated scaled harmonic frequencies of the carbonyl-bound water OH stretch of structures **III** and **IV** (3428 and 3461 cm^{-1}, respectively) reflect the same ordering as observed experimentally for MEL−W_1 A and B (3441 and 3490 cm^{-1}).

The RIDIR spectra of MEL−W_1 Y and Z are shown in parts c and d of Figure 6, respectively. As stated previously, the intense, broad transitions in W_1 Y (3457 cm^{-1}) and Z (3464/3460 cm^{-1}) are consistent with C═O bound water structures, based on a comparison of these clusters with MEL−W_1 A, MEL−W_1 B, TFA−W_1, and tropolone−W_1. We know that the water molecule is participating in the MEL−W_1 Y and Z complexes as a single donor, based on the presence of a free OH stretch at 3718 cm^{-1}. By far the most striking feature of the RIDIR spectra of MEL−W_1 Y and Z is the lack of a free indole NH stretch at ∼3525 cm^{-1}. The free amide NH stretch fundamental, which occurs at 3480−3495 cm^{-1} in the *trans*-amide MEL A−C monomers, has also moved. In their place, sharp, weak transitions flank the OH···O═C band, which are probably the shifted indole NH and amide NH stretch fundamentals (Table 2).

Based on the shift of the indole NH stretch from its "free" position, it seems likely that MEL−W_1 Y and Z incorporate the water molecule as a bridge that links the amide carbonyl and the indole NH sites. The indole NH group serves as a H-bond donor, thereby lowering the frequency of its NH stretch fundamental. Water bridging from a H-bonding site on a flexible side chain to the indole NH has been observed in the 1:2 and 1:3 tryptamine−$(water)_n$ clusters.[22] In tryptamine, the ethylamine side chain is not quite long enough to form a bridge between the indole NH and the amino group with a single water molecule.

The formation of a C═O···HO···HN (indole) bridge still does not account for the apparent shift in the amide NH stretch in

TABLE 2: Summary of the Important Spectroscopic Characteristics of the Observed Melatonin−(Water)$_n$ Clusters[a]

species	S_0-S_1 origin	electronic| frequency shift[b]	key vibronic transitions[c]	infrared transitions: indole NH	infrared transitions: amide NH	infrared transitions: water OH[d]	structural assignment[e]
				MEL Monomer			
A	32614		33, 502, 715/722	3523	3482		Gpy(*trans*-in)/anti
B	32621		41, 506, 686	3525	3494		Anti(*trans*-out)/anti
C	32795			3524	3483		Gph(*trans*-in)/anti
D	32483			3523	3422		Gph(*cis*-in)/anti
E	32432			3523	3535		
				MEL−W_1			
A	32442	MEL(A)-172	42, 45, 59 500, 517	3525	3479	3717(F), 3441(OH···O=C)	**III** (C=O bound to Mel A)
B	32956	MEL(B)+335		3527	3494	3716(F), 3490(OH···O=C)	**IV** (C=O bound to Mel B)
Y	32842			3437(?)	3415(?)	3718(F), 3457(OH···O=C)	C=O···HO···HN(Ind) cis amide(?)
Z	32673		52, 104, 251	3498(?)	3444(?)	3718, 3464/60(OH···O=C)	C=O···HO···HN(Ind) cis amide(?)
				MEL−W_2			
Y	32814	MEL−W_1(Y)-28		Part of bridge	3422(?)	3724(F), 3721(F) 3408(B), 3322(B), 3226(B)	C=O···HO···HO···HN(Ind) cis amide(?)
Z	32629	MEL−W_1(Z)-44	52, 104	Part of bridge	3462(?)	3725(F), 3717(F) 3403(B), 3337(B), 3228(B)	C=O···HO···HO···HN(Ind) cis amide(?)

[a] Reported in wavenumbers (cm^{-1}). [b] The shift of the S_0-S_1 origin from the corresponding origin in the indicated species. [c] Relative frequencies of vibronic transitions above the S_0-S_1 origin. [d] The water OH stretch transitions are labeled as free (F), carbonyl bound (OH···O=C) or bridge (B) fundamentals. The bridge fundamentals connect the indole NH to the amide carbonyl. In MEL−W_2, the bridge fundamentals incorporate the indole NH stretch fundamental. [e] Tentative assignments are labeled by a question mark (?).

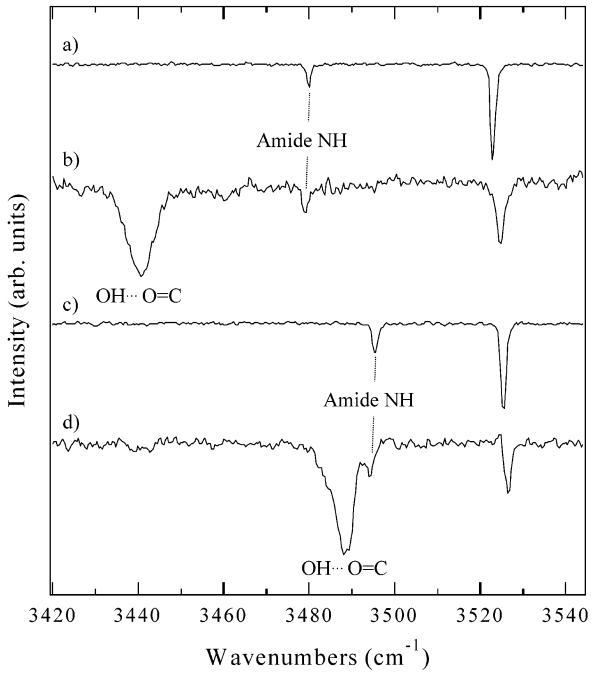

Figure 7. Close-up RIDIR scans showing the close correspondence between the amide NH stretch fundamentals of (a and b) MEL A and MEL−W_1 A and MEL B and (c and d) MEL−W_1 B.

the MEL−W_1 Y and Z clusters from their expected positions based on the *trans*-amide monomer spectra. One plausible solution is to assign these complexes to W_1 structures built off of *cis*-amide MEL monomers. It was previously determined that two of the five MEL conformers, MEL D and E, present in the expansion prior to introduction of water are *cis*-amide in nature (Figure 1). In the cis configuration, the amide NH stretch is red-shifted from its "free" position near 3490 cm^{-1} (MEL B) to 3420 cm^{-1} in MEL D and 3435 cm^{-1} in MEL E,[3] which is in the same region that the new transitions appear in MEL−W_1 Y and Z. One is tempted to make an association of MEL−W_1 Y and Z with MEL D and E. However, neither the spectroscopy nor the calculations can distinguish between low-lying *cis*-amide candidates, and we have chosen not to draw such a conclusion.

In the assignment process, the calculations have been used only to guide our thinking. A comparison of the structural deductions from Table 2 with the calculated MEL−W_1 complexes (Table 1 and Figure 3) shows that several of the structures computed to be lowest in energy (e.g., structures **I** and **II**) are not clearly assignable to any of the observed MEL−W_1 complexes. It would appear that neither the relative energies nor the vibrational frequencies are accurate enough to provide definitive assignments based on the calculations. The calculated harmonic vibrational frequencies and infrared intensities of structures **I**−**XII** are included in the Supporting Information, together with an analysis of these spectra in light of the experimental data.

E. RIDIRS of MEL−W_2. The RIDIR spectra of MEL−W_2 Y and Z are shown in Figure 8a,b, respectively. Two free OH stretches are observed in the RIDIR spectra of MEL−W_2 Y at 3724 and 3721 cm^{-1} and MEL−W_2 Z at 3725 and 3717 cm^{-1}, so as in the W_1 clusters, each water molecule in the W_2 clusters acts as a single-donor. In the RIDIR spectra of both MEL−W_2 Y and Z, the indole NH stretch is moved from its 'free' position at 3525 cm^{-1} and there are three intense, broad transitions between 3210 and 3400 cm^{-1}.

The MEL−W_2 Y and Z RIDIR spectra are consistent with formation of W_2 bridges that join the carbonyl donor and indole NH acceptor sites of MEL, thereby producing the three intense, broad bands between 3210 and 3400 cm^{-1} and shifting the indole NH stretch from its "free" position. The pattern of the bridge fundamentals (two closely spaced bands above 3300 cm^{-1} and a third near 3200 cm^{-1}) is similar in both clusters. In addition, in both MEL−W_2 Y and Z, the middle frequency bridge fundamental is the most broad of the three. Finally, in both W_2 species, the lowest energy bridge fundamental appears

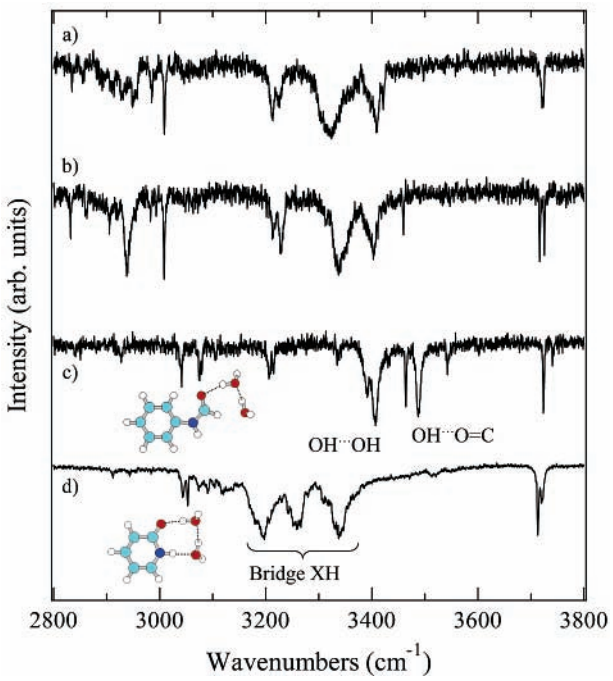

Figure 8. RIDIR spectra of (a) MEL−W_2 Y, (b) MEL−W_2 Z, (c) carbonyl-bound *trans*-formanilide−W_2, and (d) 2-pyridone−W_2. The structures of TFA−W_2 and 2PYR−W_2 are shown as insets. The latter two spectra are useful comparisons with the MEL−W_2 spectra, showing the spectroscopic consequences of water dimer bound only to the carbonyl of an amide (TFA−W_2), and a water dimer bound across the constrained *cis*-amide linkage of 2PYR−W_2. See the text for further discussion.

as two overlapping transitions, at 3213/3226 cm^{-1} in W_2 Y and 3212/3228 cm^{-1} in W_2 Z. It is likely that this bridge transition is in Fermi resonance with the overtone of the water bending vibration. The water bend overtone is also observed in the RIDIR spectrum of the A conformer of IPA−W_2 [22] at 3195 cm^{-1} and in TFA−W_2[21] at 3206/3215 cm^{-1}. These overtones are lower in frequency and somewhat weaker than the transitions in MEL−W_2 Y and Z, suggesting that the overtone of the water bend is pushed up in frequency and gains intensity from Fermi resonance with the third bridge vibration in the MEL−W_2 clusters.

Further evidence for the assignment of the MEL−W_2 Y and Z clusters to bridge structures is based upon comparison of the infrared spectra of these clusters with those of TFA−W_2 and 2-pyridone−W_2 (Figure 8c,d). The W_2 clusters formed with 2-pyridone[16] (PYR) and TFA[21] can be taken as two limiting cases of the water dimer in different solute−solvent environments. The spectrum of TFA−W_2 (Figure 8c**)** was recorded in our laboratory, but is essentially identical to that of Robertson.[21] In PYR−W_2 (Figure 8d), the water molecules bridge across the *cis*-amide group, resulting in a collection of three extremely broad, red-shifted, intense bridge fundamentals that are in-phase and out of phase combinations of the water OH and PYR NH stretches. The H-bonds formed in the PYR−W_2 bridge are cooperatively strengthened by the aromatic ring that joins the donor and acceptor sites, producing strong H-bonds with substantial frequency shifts. In contrast, TFA−W_2 (Figure 8c) cannot form a bridge structure due to the trans configuration of the amide group. Instead, the water dimer in this conformer of TFA−W_2 is bound only to the carbonyl oxygen by a single H-bond,[21] resulting in two fairly intense, broad transitions that are less strongly shifted (3407 and 3487 cm^{-1}), assigned as the H-bonded OH···OH stretch and the OH···O=C stretch. The amide NH stretch is not involved in any H-bonds and remains sharp and at its frequency in the TFA monomer. The overtone of the water bend is very weak and lower in frequency than the analogous band in MEL−W_2. We see that the H-bonds found in MEL−W_2 Y and Z are stronger than those found in TFA−W_2 based on the larger red-shift, intensity, and breadth of the infrared transitions, in keeping with the MEL−W_2 bridge assignment. Furthermore, the lack of the indole NH stretch at its "free" position is a strong indicator that the W_2 clusters of MEL are in fact bridges to this site. On the bases of vibrational frequency shifts, it appears that the MEL−W_2 Y and Z bridges fall somewhere between a water dimer bound only to a C=O and a water dimer that is strongly bound to two distinct H-bonding bridge sites.

Recall that, based on their similar electronic frequency shifts and vibronic structure in the R2PI spectra, we have already tentatively assigned MEL−W_2 Y to a structure built off of MEL−W_1 Y and MEL−W_2 Z to a structure built off of MEL−W_1 Z. Such an association is strengthened further by the comparison of their infrared spectra (Figure 6c,d versus Figure 8a,b). First, the CH stretching fundamentals within each "family" are very similar to one another, and somewhat distinct from the other two MEL−W_1 complexes (Figure 6a,b). Second, the indole NH stretch is moved from its free position of 3525 cm^{-1} in all of these clusters. As in the W_1 Y and Z clusters, the amide NH stretch fundamental of the W_2 Y and Z clusters is hard to locate with certainty. Tentative assignments (Table 2) are made to weak, sharp bands at 3422 cm^{-1} in the spectrum of MEL−W_2 Y and 3462 cm^{-1} in MEL−W_2 Z. The former band has a close analogue in the 3415 cm^{-1} band in MEL−W_1 Y. The low frequencies of these amide NH stretch fundamentals are most consistent with *cis*-amide MEL structures in the MEL−W_2 Y and Z clusters.

IV. Discussion

A. The Effect of Water on the Conformational Preferences of Melatonin. The complexation of water molecule(s) to melatonin has several important effects on the conformational preferences of melatonin. First, it changes the number of conformations of MEL with significant population. While there are five observed conformations of the MEL monomer (three *trans*-amides and two *cis*-amides), four conformers of MEL−W_1 were detected, and only two of MEL−W_2. The relative energies of the conformations and the heights of the barriers separating them are both effected in significant ways by the presence of even a single water molecule bound to MEL at the carbonyl site. It would be very interesting to map out the potential energy surface for MEL both with and without water using state-of-the-art ab initio methods in order to understand these changes more deeply.

Second, in those conformations that are observed, the relative abundances of the conformations can be changed. For instance, the MEL−W_1 A and B complexes are both derived from MEL monomer conformations with significant population in the expansion (MEL A and B, respectively). Furthermore, the MEL−W_1 A complex with the largest population derives from the MEL monomer conformation with the largest population. However, based on the relative R2PI signals, the MEL−W_1 A cluster has a population that is about 10 times larger than that of any other W_1 species observed in the expansion, suggesting that water preferentially binds to MEL A over other conformations.

An even more dramatic example of conformational population shift is suggested by the results on MEL−W_2, where the preference for *trans*- over *cis*-amides appears to be reversed in

the presence of a water dimer bridge. In the case of the MEL monomer, we have observed a small amount of population trapped in *cis*-amide configurations, due to the large barrier to *cis/trans* isomerization (~15 kcal/mol). It seems likely that the process by which a single water molecule complexes to the *cis*-amide monomers does not provide enough energy to isomerize, and therefore a small fraction of the population is trapped as *cis*-amide W_1 clusters. From this perspective, it is not surprising that two of the minor MEL−W_1 complexes (labeled Y and Z), have amide NH stretch fundamentals that are most consistent with assignment to *cis*-amide MEL conformations. These complexes have infrared spectra consistent with water bridging between the carbonyl group H-bond acceptor and the indole NH H-bond donor sites.

On the bases of such arguments, one would anticipate that, in the MEL−W_2 clusters, both *trans*- and *cis*-amide W_2 clusters would be observed. However, only two W_2 clusters were detected. These have hydrogen bonding topologies that are similar to one another, reflecting a water dimer bridge between the C═O and indole N−H groups. More surprising is our tentative conclusion, based on the spectral data, that both structures most likely have *cis*-amide MEL conformations. One might have thought that a driving force for *cis*-amide formation would be to facilitate a water molecule acting as a bridge between the adjacent amide NH and the amide C═O groups in a *cis*-amide, as occurs in 2-pyridone−$(water)_n$ clusters.

However, the suggestion arising out of our data is that the isomerization to a *cis*-amide facilitates the formation of a bridge between the amide carbonyl and the indole N−H. In these cases where the flexible side-chain containing the amide group is too short to form a strong bridge with the indole NH, the formation of the *cis*-amide may enable the flexible side chain to reorient into a better configuration for water bridge formation. This general idea is supported by the energy of structure **II**, which is only 0.8 kcal/mol less stable (Table 1) than the most strongly bound *trans*-amide structure (**I**), suggesting a closing of the energy gap between cis and trans amides when a single water molecule is present. A more decisive experimental verification of this suggestion would be highly desirable, since it represents an extreme example of water redirecting the conformational preferences of a flexible side chain, even in the presence of substantial barriers to isomerization in the absence of water.

The assignment of the MEL−W_2 Y and Z to bridges built off the weakly populated MEL−W_1 Y and Z begs the question as to why these are the only W_2 clusters observed. There are two possibilities. First, formation of the MEL−W_2 bridge could provide sufficient energy to drive all of the population into these two minima. If the deduction that these bridges involve *cis*-amide MEL conformations is correct, this would necessitate converting all of the *trans*-amide MEL conformers into *cis*-amides, a process that has a barrier of about 15 kcal/mol[23−25] in the monomer. The isomerization barrier may be reduced in the presence of water, and formation of the water bridge might deposit the energy needed to isomerize into the cluster. Alternatively, it is possible that the *trans*-amide−W_2 clusters were present in the expansion, but were not observed, either by virtue of unusually large electronic frequency shifts, signal dilution from spectral congestion, shortened S_1-state lifetimes, or poor Franck−Condon factors to the ion.

B. The Effects of Water Binding on the Electronic Frequency Shifts. In the electronic spectroscopy of MEL−W_1 A and B, we observe large frequency shifts from the MEL A and B monomer origins, respectively. These frequency shifts are in the opposite direction (−172 cm^{-1} for A and +335 cm^{-1} for B, Table 2) even though the water is bound at the same site on the respective monomers and is seemingly quite far removed from the indole π cloud. The RIDIR spectra of the MEL−W_1 A and B prove that in both cases the water molecule is bound only to the carbonyl group. The position of the water molecule relative to the indole ring seems to cause this unusual electronic frequency shift behavior. In MEL−W_1 A (structure **III**), the water molecule is on the exterior of the side chain, very far from the indole chromophore. In MEL−W_1 B (structure **IV**), the water molecule is located on the interior of the side chain, closer to the indole π cloud, and is calculated to be 3.56 angstroms from the carbon atom of the methoxy group. The presence of the methoxy group on the indole ring is responsible for a dramatic stabilization of the S_1-state of MEL and 5-methoxyindole relative to indole (producing an S_0-S_1 origin red-shifted from indole by ~2600 cm^{-1}).[3,26] It is likely that the proximity of the water to the methoxy group destabilizes the S_1-state of MEL−W_1 B relative to MEL B, resulting in this unexpected electronic frequency shift behavior.

V. Acknowledgments

The authors gratefully acknowledge support from the National Science Foundation Experimental Physical Chemistry program via a 2 year extension to Grant CHE-9728636, and to the donors of the Petroleum Research Fund, administered by the American Chemical Society.

Supporting Information Available: Further details of the conformational assignments of MEL−W_1 and MEL−W_2 using the harmonic vibrational frequencies and infrared intensities calculated at the DFT Becke3LYP/6-31+G*(5d) level of theory as a point of comparison with experiment. This material is available free of charge via the Internet at http://pubs.acs.org.

References and Notes

(1) Godfrey, P. D.; Brown, R. D.; Rodgers, F. M. *J. Mol. Struct.* **1996**, *376*, 65.
(2) Godfrey, P. D.; Brown, R. D. *J. Am. Chem. Soc.* **1998**, *120*, 10724.
(3) Florio, G. M.; Christie, R. A.; Jordan, K. D.; Zwier, T. S. *J. Am. Chem. Soc.* **2002**, *124*, 10236.
(4) King, M.; Scaiano, J. C. *Photochem. Photobiol.* **1997**, *65*, 538.
(5) Rath, M. C.; Mahal, H. S.; Mukherjee, T. *Photochem. Photobiol.* **1999**, *69*, 294.
(6) Creed, D. *Photochem. Photobiol.* **1984**, *39*, 537.
(7) Zwier, T. S. *J. Phys. Chem. A* **2001**, *105*, 8827.
(8) Cannington, P. H.; Ham, N. S. *J. Electron Spectrosc. Relat. Phenom.* **1983**, *32*, 139.
(9) Becke, A. D. *J. Chem. Phys.* **1993**, *98*, 5648.
(10) Lee, C.; Yang, W.; Parr, R. G. *Phys. Rev. B* **1988**, *37*, 785.
(11) Frisch, M. J.; Pople, J. A.; Binkley, J. S. *J. Chem. Phys.* **1984**, *80*, 3265.
(12) Frisch, M. J.; Trucks, G. W.; Schlegel, H. B.; Scuseria, G. E.; Robb, M. A.; Cheeseman, J. R.; Zakrzewski, V. G.; Montgomery, J. A.; Stratmann, R. E.; Burant, J. C.; Dapprich, S.; Millam, J. M.; Daniels, A. D.; Kudin, K. N.; Strain, M. C.; Farkas, O.; Tomasi, J.; Barone, V.; Cossi, M.; Cammi, R.; Mennucci, B.; Pomelli, C.; Adamo, C.; Clifford, S.; Ochterski, J.; Petersson, G. A.; Ayala, P. Y.; Cui, Q.; Morokuma, K.; Malick, D. K.; Rabuck, A. D.; Raghavachari, K.; Foresman, J. B.; Cioslowski, J.; Ortiz, J. V.; Baboul, A. G.; Stefanov, B. B.; Liu, G.; Liashenko, A.; Piskorz, P.; Komaromi, I.; Gomperts, R.; Martin, R. L.; Fox, D. J.; Keith, T.; Al-Laham, M. A.; Peng, C. Y.; Nanayakkara, A.; Gonzalez, C.; Challacombe, M.; Gill, P. M. W.; Johnson, B.; Chen, W.; Wong, M. W.; Andres, J. L.; Gonzalez, C.; Head-Gordon, M.; Replogle, E. S.; Pople, J. A. *Gaussian 98*, revision A.7; Gaussian, Inc.: Pittsburgh, PA, 1998.
(13) Carney, J. R.; Dian, B. C.; Florio, G. M.; Zwier, T. S. *J. Am. Chem. Soc.* **2001**, *123*, 5596.
(14) Held, A.; Pratt, D. W. *J. Am. Chem. Soc.* **1993**, *115*, 9708.
(15) Matsuda, Y.; Ebata, T.; Mikami, N. *J. Chem. Phys.* **1999**, *110*, 8397.
(16) Florio, G. M.; Gruenloh, C. J.; Quimpo, R. C.; Zwier, T. S. *J. Chem. Phys.* **2000**, *113*, 11143.
(17) Carney, J. R.; Zwier, T. S.; Fedorov, A. V.; Cable, J. R. *J. Phys. Chem. A* **2001**, *105*, 3487.

(18) Callis, P. R.; Vivian, J. T.; Slater, L. S. *Chem. Phys. Lett.* **1995**, *244*, 53.
(19) Frost, R. K.; Hagemeister, F. C.; Arrington, C. A.; Schleppenbach, D.; Zwier, T. S.; Jordan, K. D. *J. Chem. Phys.* **1996**, *105*, 2605.
(20) Dickinson, J. A.; Hockridge, M. R.; Robertson, E. G.; Simons, J. P. *J. Phys. Chem. A* **1999**, *103*, 6938.
(21) Robertson, E. G. *Chem. Phys. Lett.* **2000**, *325*, 299.
(22) Carney, J. R.; Zwier, T. S. *Chem. Phys. Lett.* **2001**, *341*, 77.
(23) Scherer, G.; Kramer, M. L.; Schutkowski, M.; Reimer, U.; Fischer, G. *J. Am. Chem. Soc.* **1998**, *120*, 5568.
(24) Schiene-Fischer, C.; Fischer, G. *J. Am. Chem. Soc.* **2001**, *123*, 6227.
(25) Li, P.; Chen, X. G.; Shulin, E.; Asher, S. A. *J. Am. Chem. Soc.* **1997**, *119*, 9, 1116.
(26) Huang, Y.; Sulkes, M. *J. Phys. Chem.* **1996**, *100*, 16749.